tvst

Methods

Microperimetry Hill of Vision and Volumetric Measures of Retinal Sensitivity

Amandeep Singh Josan[1,2], Thomas M. W. Buckley[2], Laura J. Wood[1,2], Jasleen K. Jolly[1,2], Jasmina Cehajic-Kapetanovic[1,2], and Robert E. MacLaren[1,2]

[1] Nuffield Laboratory of Ophthalmology, Nuffield Department of Clinical Neurosciences, University of Oxford, Oxford Biomedical Research Centre, Oxford, UK
[2] Oxford Eye Hospital, Oxford University Hospitals NHS Foundation Trust, Oxford, UK

Correspondence: Amandeep Singh Josan, Nuffield Laboratory of Ophthalmology, Level 6 John Radcliffe Hospital West Wing, Headley Way, Headington, Oxford OX3 9DU, UK. e-mail: enquiries@eye.ox.ac.uk

Received: July 15, 2020
Accepted: May 5, 2021
Published: June 10, 2021

Keywords: microperimetry; hill of vision; volume; retinal function; functional imaging

Citation: Josan AS, Buckley TMW, Wood LJ, Jolly JK, Cehajic-Kapetanovic J, MacLaren RE. Microperimetry hill of vision and volumetric measures of retinal sensitivity. Transl Vis Sci Technol. 2021;10(7):12, https://doi.org/10.1167/tvst.10.7.12

Purpose: Mean retinal sensitivity is the main output measure used in microperimetry. It is, however, of limited use in patients with poor vision because averaging is weighted toward zero in those with significant scotomas creating an artificial floor effect. In contrast, volumetric measures avoid these issues and are displayed graphically as a hill of vision.

Methods: An open-source program was created to manipulate raw sensitivity threshold data files obtained from MAIA microperimetry. Thin plate spline interpolated heat maps and three-dimensional hill of vision plots with an associated volume were generated. Retrospective analyses of microperimetry volumes were undertaken in patients with a range of retinal diseases to assess the qualitative benefits of three-dimensional visualization and volumetric measures. Simulated pathology was applied to radial grid patterns to investigate the performance of volumetric sensitivity in nonuniform grids.

Results: Volumetric analyses from microperimetry in *RPGR*-related retinitis pigmentosa, choroideremia, Stargardt disease, and age-related macular degeneration were analyzed. In simulated nonuniform testing grids, volumetric sensitivity was able to detect differences in retinal sensitivity where mean sensitivity could not.

Conclusions: Volumetric measures do not suffer from averaging issues and demonstrate superior performance in nonuniform testing grids. Additionally, volume measures enable detection of localized retinal sensitivity changes that might otherwise be undetectable in a mean change.

Translational Relevance: As microperimetry has become an outcome measure in several gene-therapy clinical trials, three-dimensional visualization and volumetric sensitivity enables a complementary analysis of baseline disease characteristics and subsequent response to treatment, both as a signal of safety and efficacy.

Introduction

Fundus-tracked perimetry, known as microperimetry, is being widely adopted in eye hospitals and research environments to aid in the diagnosis and monitoring of a variety of ocular diseases that affect the central retina. Microperimetry has also been used as an outcome measure in various clinical trials involving novel treatments for inherited and age-related retinal diseases and age-related diseases such as choroideremia, retinitis pigmentosa, and age-related macular degeneration [Clinicaltrials.gov ref: NCT02407678, NCT03116113, NCT03846193]. Advancements in retinal imaging techniques in combination with microperimetry permit accurate structure-function correlations to be made.

The standard output of the MAIA microperimeter (Macular Integrity Assessment; CenterVue, Padova, Italy) includes graphical representations of the point thresholds (or pointwise sensitivities) overlaid onto an image of the fundus indicating the retinal locations of each stimulus presented (Fig. 1A). The sensitivity map is also displayed with radial interpolation

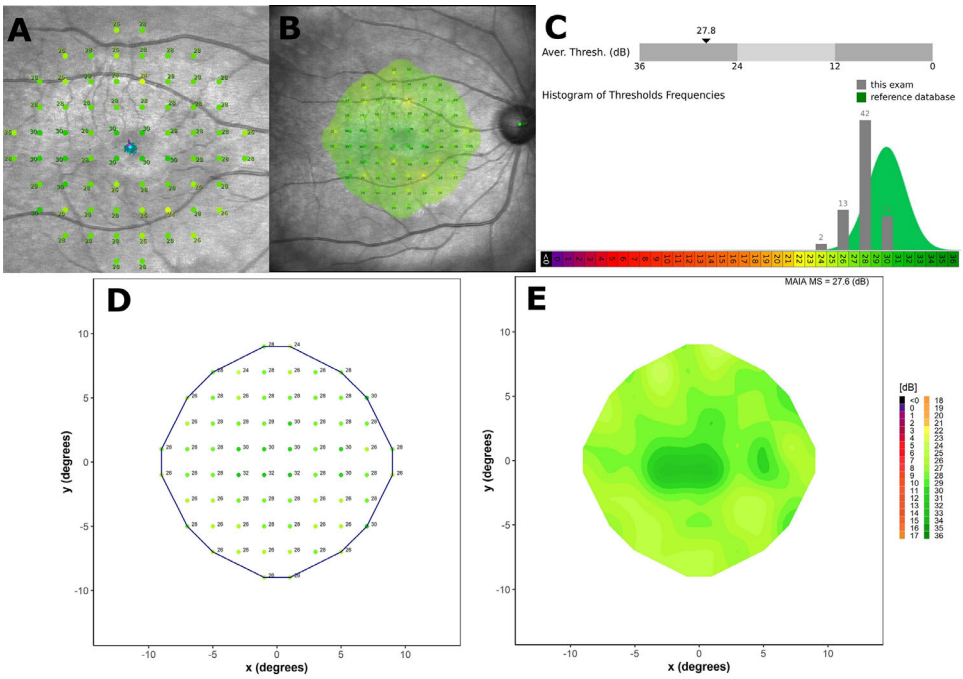

Figure 1. Top row: An example of a standard output given by the MAIA microperimeter for a healthy subject. (**A**) Point threshold values overlayed onto a fundus image. (**B**,) Heatmap output using a radial interpolation with point threshold values. (**C**) Histogram of point threshold values and a mean sensitivity value for all points. (**D**,) Point sensitivity output of custom program and boundary using a convex hull about the outermost tested points. (**E**) Heatmap generated using thin plate spline interpolation of point sensitivities.

of each point displayed as heat map (Fig. 1B). The final MAIA output relevant to this study is a calculation of the average threshold (mean sensitivity) of all points alongside a histographic representation of point threshold sensitivities (Fig. 1C). Here, the mean sensitivity is given by the average of all point threshold values.

Threshold values are given in the range −1 dB to 36 dB with 0 dB to 36 dB the dynamic range of the stimuli luminances and −1 dB representing instances when the brightest stimulus (0 dB) is not seen. This negative decibel value is a proxy value for a hypothetically brighter stimulus (by one log unit than the 0 dB stimulus) that cannot be achieved by the MAIA machine and represents the "floor effect" generated by a limitation of the devices' brightness capabilities. It is used as a tool to represent areas of sensitivity too low to be measured by the limits of the microperimeter machine and not an actual measure of the retinal sensitivity at that location.

The primary outcome from the MAIA microperimeter is the mean sensitivity, given in decibels (dB), which describes the average retinal sensitivity within the given visual field area. This measure has several positive attributes; it is a single value; simple to understand; and has a wide range of possible values providing a reasonable sensitivity to detect changes in retinal function. There are, however, some notable drawbacks inherent to this measure. The process of averaging sacrifices localized information, whereby large areas of moderate sensitivity gains maybe outweighed by localized losses in other areas. In addition, in advanced disease where the size of scotoma is larger than the remaining area of functional retina, the mean sensitivity is weighted heavily towards zero decibels. This creates an additional floor effect (separate from the floor effect caused by a limited dynamic range of the device) because of averaging methods in patients close to end-stage disease whereby the mean sensitivity returns 0 dB despite remaining sensitive retinal locations. This has implications for monitoring disease progression and detecting safety and efficacy signals for established or novel treatments. Finally, average values without weighting consideration may only have validity within regular equidistant spaced testing patterns. For irregular or radial grid patterns with centrally condensed points, averaging significantly weights in favour of points located in more densely arranged areas and may underestimate the potential sensitivity in regions sampled by fewer points. This last limitation has significant implications for accuracy and efficiency that maybe overcome by methods of spatial weighting such as Voronoi mosaic areas[1]; however, these weighted averages do not address the issue of the floor effect

caused by averaging in advanced disease discussed earlier.

These drawbacks are overcome by consideration of a "hill of vision," a concept first introduced by Traquair in 1927.[2] A volumetric measure of the hill of vision, which is a measure of the "total amount" of sensitivity within a given visual field area, may be calculated in physical units of decibel-steradians[3,4] or decibel-degrees squared, and represents both the degree and extent of sensitivity in the region of interest. Volumetric data and three-dimensional representations in perimetry have been used by Weleber et al.[3,5] using a custom program termed visual field modeling and analysis (VFMA), as an outcome measure in patients undergoing gene therapy trials.[3,5] These include a clinical trial to investigate potential treatments for autosomnal dominant retinitis pigmentosa[6] and studies of Goldmann kinetic perimetry in retinitis pigmentosa.[7] Volume and slope of the hill of vision metrics have also been used to investigate structure-function correlations in autosomnal dominant retinitis pigmentosa.[8] VFMA and volumetric approaches have been applied to microperimetry assessments in several instances; Tanna et al.[9] in longitudinal assessment of retinal sensitivity in patients with childhood-onset Stargardt disease; Mehat et al.[10] in clinical trials for stem cell treatment in advanced Stargardt disease; and Dimopoulos et al.[11] in investigating the use of customized grids in patients with choroideremia. A volumetric measure, with the the notable benefit of eliminating the need for averaging methods, is limited only by the true floor effect of the microperimter device rather than an averaging value floor effect. These are of particular importance in gene therapy trials where patients may be near end-stage visual function. Novel treatments may be targeted to highly localized regions with gains in some areas offset by losses caused by natural disease progression in areas that remain untreated. In addition, an interactive three-dimensional visualization of a hill of vision may aid in interpretation of changes when monitoring disease progression in comparison to standard two-dimensional sensitivity heat map outputs from microperimeter devices. There are known age-related changes in perimetry. However, investigations into age-related normative values in microperimetry are limited[12,13] and therefore are not yet a part of the standard MAIA output. Historically, volumetric data have not been commonly used due to the difficulties in coding custom programs for the task of three-dimensional rendering. The widespread adoption of R programming language[14] along with several open source packages used within R have made this task far simpler and within reach for eye research departments.

We introduce a web application and an open-source code within R programming language (v3.6.3) which allows for the three-dimensional visualization of the hill of vision generated by post-analysis of a standard output raw data file from MAIA microperimeter. Subsequently, this allows calculation of a microperimetry volume, providing a measure of extent and degree of sensitivity of the centrally tested field that is independent to the mean sensitivity. We present examples of its application in several acquired and inherited retinal diseases to demonstrate the qualitative benefits of three-dimensional visualization before defining the relationship between the mean sensitivity and sensitivity volumes. We then apply volumetric analysis to microperimetry results from a subject treated as part of a recently reported phase I/II gene-therapy trial for *RPGR*-related retinitis pigmentosa[15] to demonstrate its potential utility as a clinical trial outcome measure.

Methods

Data Preparation

Generation of heat maps and three-dimensional surface plots of the hill of vision were carried out in R,[14] a freely available open source statistical programming package. All plots were generated on a standard Dell (Intel i7) laptop with no special modifications. The complete code, with an example input file, can be downloaded directly from a Github repository (https://github.com/amanasj/MAIA3D) or can be installed as an R package using the command "install_github('amanasj/mp3d')" and the package called using "library(mp3d)." Using this code, with some minor data preparation, we used the exported threshold text data files (threshold.txt) from the MAIA microperimeter to create a three-dimensional plot using interpolation and three-dimensional graphical packages. Each plot is rendered and displayed within a few seconds and requires minimal processing power. Alternatively, A web application (https://ocular.shinyapps.io/MAIA3D/) can be used to upload a raw threshold.txt file to automatically generate an interactive three-dimensional hill of vision.

In preparing the raw data files for graphical representation, we identifed several issues with the numerical output from MAIA. Firstly those points that are seen using only the brightest stimulus (0 dB) do not contribute toward the mean sensitivity, or crucially, volume measures. We therefore elected to convert each 0 dB value to an arbitrary nominal value of 0.1dB so as

to "reward" a "just seen" point at maximum brightness. Secondly, non-seen point values of −1dB representing the floor effect of the machine are incorporated into the calculation of mean sensitivity which only serves to exaggerate averaging floor effects by negatively scoring non-seen points. To restate, in calculating mean sensitivity, the inclusion of −1 dB values drives the mean sensitivity value artificially to towards zero. We therefore convert all −1 dB (non-seen) values to 0 dB. Our treatment of "non-seen" points follows the methodology used in static-automated perimetry such as in the Octopus 900.[16]

The complete code as given in the supplementary section contains comments detailing each step of the process with a brief descriptive outline of the code structure given initially. This code is optimized in its current form to only process results from the MAIA microperimeter but could, with very minor modifications, be adapted for any perimetry device.

Interpolation

Interpolation is the process of predicting values *between* two known data points. In the context of microperimetery it is a predicted line or curve between tested threshold points. It is a natural extension of the concept of extrapolation for predicting values *beyond* the range of tested data points. Interpolation seeks to model smooth transitions between tested locations and graphically display the result as heat maps. Interpolation techniques, however, are a complex field with many possible choices depending on the type of data in question. For example, interpolation of a set of data points such as the point threshold sensitivity values in microperimetry can be chosen to be a simplistic linear trend from one point to the next (first degree polynomial), quadratic (second degree polynomial) or cubic (third degree polynomial) curves. In these instances abrupt changes in gradients appear where two polynomials meet. To address this, smoothness can be increased by imposing the requirement of continuous first and second degree gradients (i.e., constant first and second degree derivatives). This acts to transition various polynomial fits resulting in smooth curves and transitions between data points. The resulting curve generated by imposing constant first and second degree gradients is called a "spline." Cubic splines are extensively used in image processing due to ease and speed of computation. Cubic splines, however, have a tendency to 'overshoot' when dealing with large changes between two point values creating undesirable artifacts adjacent to tested points. Interpolation using thin plate splines have been suggested as a more suitable option.[17] Here threshold points are treated as fixed points (knots) about which the interpolated surface is modelled as a thin plate of metal with a resistance, or minimum, bending energy associated between threshold points.[18]

Interpolation using thin plate splines in our code is performed using the *fields* package (version 10.3).[19] Two-dimensional plots are produced in *ggplot2* package (version 3.31).[20] We advise that all packages listed in the initial section of the R code provided in the supplementary section are installed. Using a MAIA threshold raw data file and the code in the supplementary section, an example point sensitivity plot can be produced (Fig. 1D). Here the tested points are bounded by the outermost points forming a convex hull. This ensures an abrupt termination of the interpolation at the outer boundary minimising potential artifacts arising from edge effects. Once interpolation is performed, ggplot2 is used to graphically display the heat map (Fig. 1E).

Volumetric Analyses

Once the MAIA data file has been interpolated into a two dimensional heatmap, three-dimentional surface plots of the hill of vision are produced using the *persp3d* function within *rgl* package (version 0.100.54).[21] Volumetric measures are calculated by a simple integration over this surface with values given in units of dB-degrees^2. Weleber et al.[3] use units of dB-Sr, with steradians (Sr) an SI unit of solid area on a spherical surface. In the context of full field kinetic perimetry, cartographic distortions arise due to translation of two-dimensional isopter plots into a measure of retinal space. For example, spherically shaped retinal scotomas or testing grid patterns appear elliptical on two-dimensional field plots.[4] Decibel-steradians are a natural unit in these instances where two- to three-dimensional conversions are neccesary for an accurate volume measure. In microperimetry, however, typically only the central 10° radius is examined, and so we consider at these eccentricities there are minimal effects of cartographic distortions.[11,22] We therefore adopt dB-degrees^2 as a more intuitive unit of volume measure with familiarity and ease of interpretation by clinicians.

Subject Cases

Retrospective analysis of microperimetry examination results from four patients with a range of retinal diseases and one healthy control subject was performed. All patients gave written informed consent and the research adhered to the tenets of the declaration of Helsinki. Microperimetry examinations

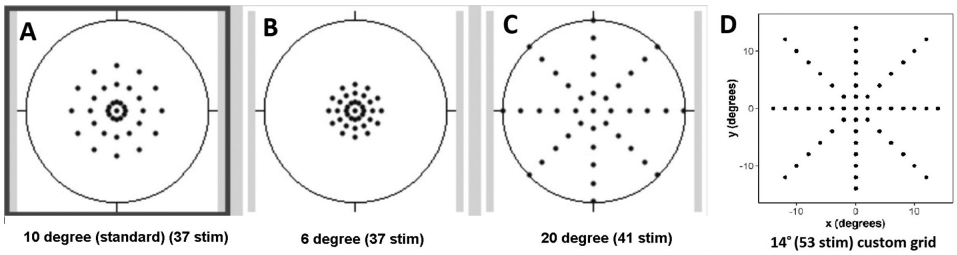

Figure 2. (**A**, **B**, **C**) Examples of preset nonuniform radial grid patterns that can be selected within the MAIA. A custom radial grid (**D**) was designed to demonstrate volumetric measures.

were carried out with the MAIA device (CenterVue, Padova, Italy) at the Oxford Eye hospital as part of screening for ongoing studies (REC reference 17/LO/1540, NCT03846193, NCT03116113). A comparison of volumetric values using our algorithm to that obtained using VFMA for each subject case was made (VFMA program supplied under a Collaborative Research Agreement by the OHSU Office of Business Collaborations and Technology Transfer, Portland, OR, USA).[3]

Perimetric Quality Control

Fixation losses were assumed to result from false-positive suprathreshold blind spot presentations (Heijl-Krakau method)[23] and those examinations with fixation losses above 30% were deemed unreliable and not included for analysis (as per MAIA operating manual). In addition, we conducted a more in-depth volumetric analysis on one patient with a confirmed diagnosis of *RPGR*-related retinitis pigmentosa who participated in a phase 2 gene therapy clinical trial, the results of which have been previously reported.[15]

Radial or Nonuniform Grid Patterns

Within the MAIA there are several alternative preset grid options to the standard 10-2 grid, some of which use nonuniform grid patterns, that is, those with irregular or nonuniform spacing between points such as radial grid patterns with a central condensation of points (Figs. 2A–2C). In addition, custom grids can be manually created with stimuli added at any desired location. Using our R code, we generated a nonuniformly spaced grid pattern (Fig. 2D) and manually input point sensitivity data to simulate two distinctly different pathological retinal sensitivity patterns. Both simulated pathologies were created to have equal mean sensitivity. The three-dimensional hill of visions were produced to investigate the performance of volumetric measures compared to the mean sensitivities.

Results

Case Studies

Three-dimensional microperimetry hill of vision plots are shown in Figure 3 and represent a normal control subject and a range of patients with confirmed ocular pathologies. Using the programming code to generate these in R (given in the supplementary section), these three-dimensional visualisations become interactive with the viewpoint altered using the computer mouse as desired. The interactive three-dimensional plots can be saved as HTML files for later viewing. The images in this article represent screenshots of those interactive plots. Results are presented with values for both mean sensitivity and volume for comparison.

Figure 4 shows longitudinal microperimetry results for a patient who underwent gene therapy of the right eye as part of a phase II trial. The results from baseline (pre-treatment) through to week 12 post-treatment have previously been reported by Cehajic-Kapetanovic et al.[15] The three-dimensional representations shown provide a more intuitive visualization and interpretation of changes in retinal function with corresponding volume measures allowing for a measure of overall retinal sensitivity utilizing the full dynamic range of the microperimetry device. At week five after treatment, an inflammatory response resulted in a temporary loss of retinal sensitivity at several locations, with mean sensitivity reporting zero decibels despite individual point sensitivities remaining. A volumetric measure, however, captures this information recording a nonzero value (analysis of data extracted from Cehajic-Kapetanovic et al.[15]). A comparison of microperimetry volume measures presented in this work from that obtained using the VFMA program is given in Supplementary Table S1 (supplementary section). Evaluation of agreement carried out using intraclass correlation coefficient (ICC) using a 2-way random effects model demonstrated excellent agreement between the two measures with an ICC of 0.99.

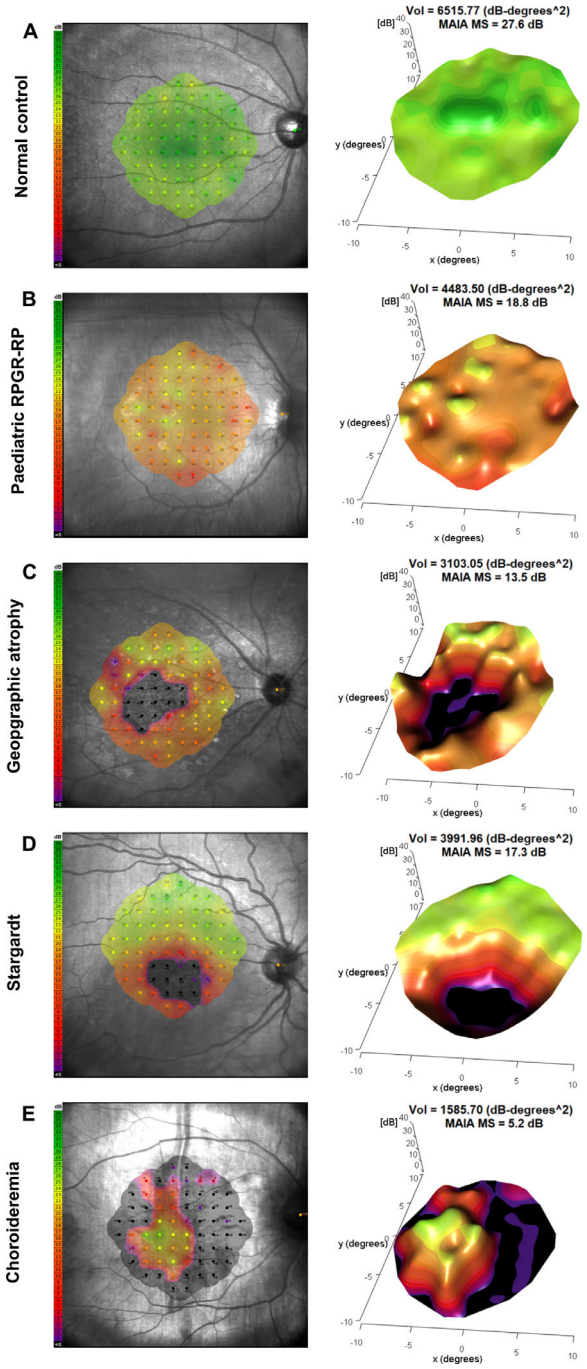

Figure 3. (**A**) Normal control patient with the standard output from MAIA showing heat map overlaid onto a fundus image (left) and a three-dimensional of hill of vision (right) using the custom program provided. Volume (vol) and mean sensitivity (MS) values are displayed. (**B**) Standard MAIA output (left) and three-dimensional hill of vision (right) for a pediatric patient with *RPGR*-related retinitis pigmentosa demonstrating an overall depression of retinal sensitivity as indicated by the warmer colors: Three-dimensional visualization demonstrates a complex structure in the sensitivity map formed by interpolation of individual point threshold sensitivities. (**C**) A patient with geographic atrophy with a central scotoma. Note on the three-dimensional hill of vision plot (right), the steep gradients superior to the central scotoma with more gradual changes inferiorly. (**D**) A patient with Stargardt disease with central macula scotoma. Here the patient has developed eccentric fixation as seen by a superior shift in grid centering. (**E**) A patient with choroideremia

←

with advanced paracentral field loss. The remaining central island retains moderate to good threshold sensitivities associated with good visual acuity. Three-dimensional visualization of the hill of vision (right) clearly reveals characteristic steep gradients across the island-scotoma border.

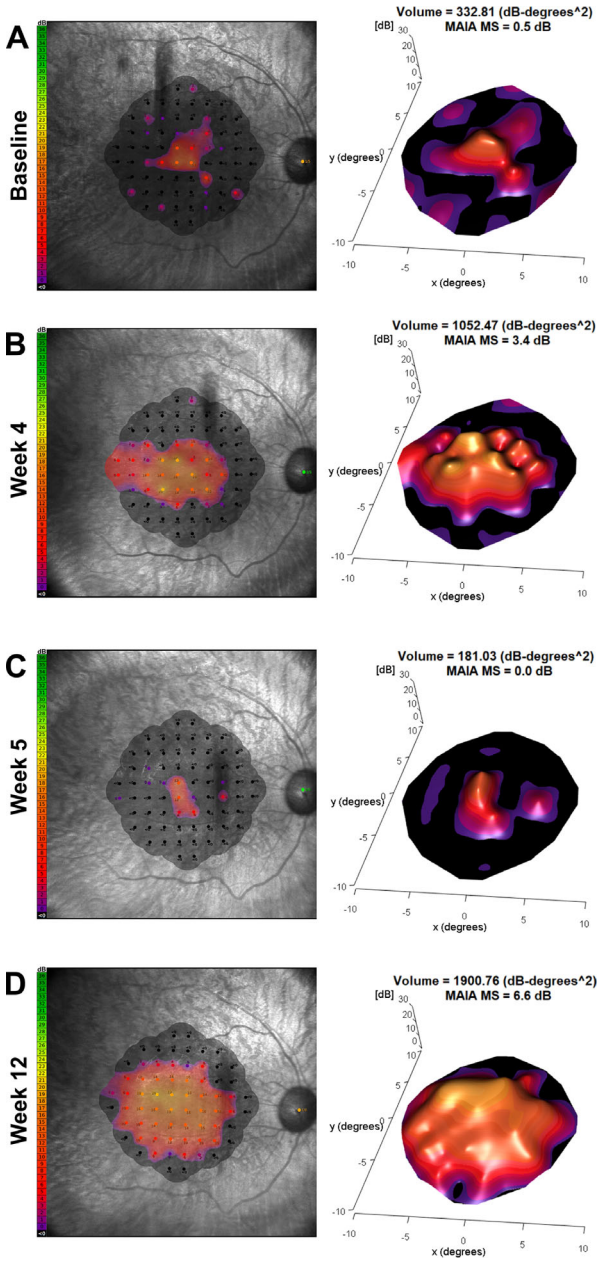

Figure 4. Microperimetry results for an *RPGR*-related retinitis pigmentosa patient who underwent gene therapy treatment in the right eye. Left: Standard output from MAIA. Right: Three-dimensional hill of vision. Increases in retinal sensitivity and field extent were interrupted by regression at week 5 (plot C) associated with inflammation which, once treated, resulted in return of microperimetry sensitivity gains. Note at week 5, the mean sensitivity given as 0 dB despite the presence of sensitive points caused by averaging of a large number of scotoma points. Volumetric data capture these point sensitivities returning a nonzero value.

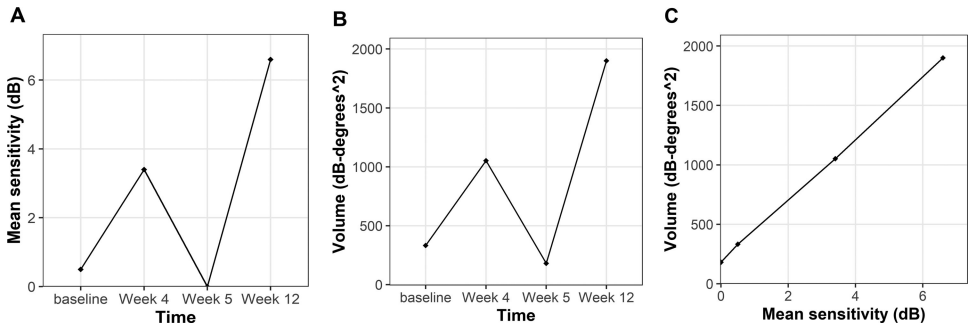

Figure 5. Microperimetry measures for the treated right eye of the *RPGR*-related RP patient shown in Figure 4. (**A**) Longitudinal data for the standard MAIA output of mean sensitivity at baseline and subsequent visits after receiving gene therapy treatment. (**B**) Hill of vision volume measure for the same time points. (**C**) Comparison of mean sensitivity and volume as retinal sensitivity measures. Note the nonzero values returned using volumetric measures.

Mean Sensitivity and Volume Comparisons

Mean sensitivity as a simple, single value measure of retinal sensitivity has a useful function in a clinical setting. Using a case study of the *RPGR*-related RP patient shown in Figure 4, for moderate to high values, average sensitivity has a good agreement with volume measures as shown in Figures 5A and 5B. Mean

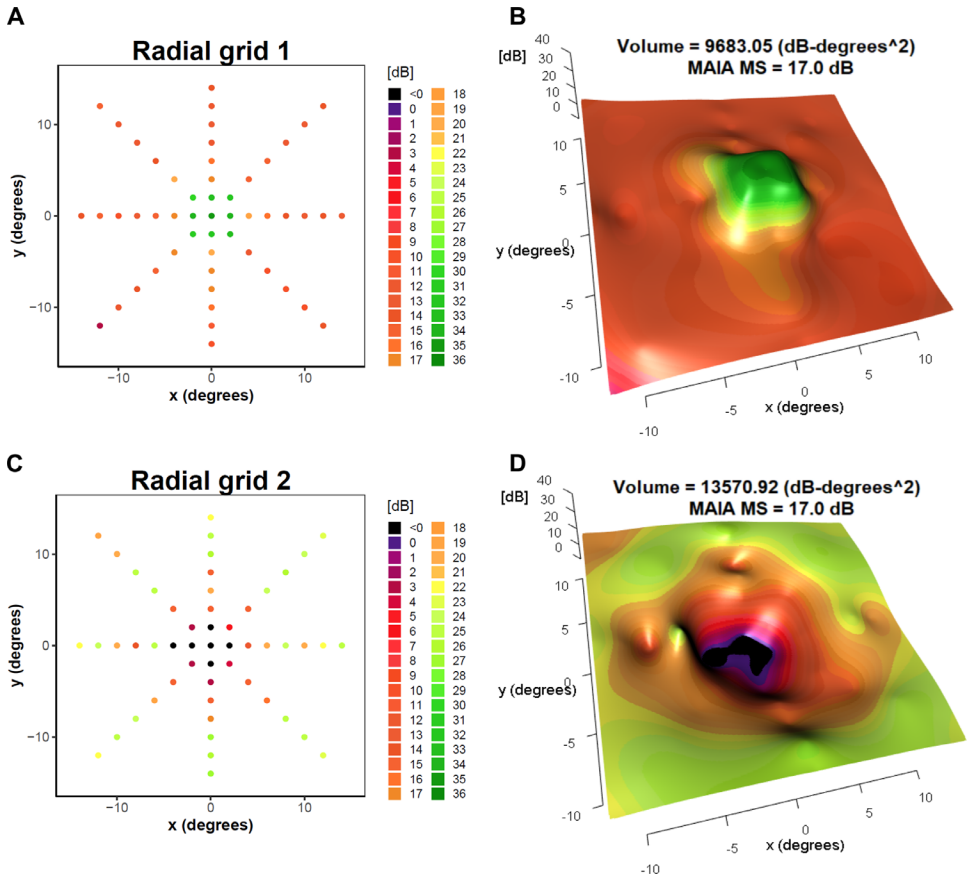

Figure 6. Custom designed radial grid patterns with simulated threshold values manually input to create distinctly different hills of vision. (**A**, **B**) The distribution of point sensitivities and the resulting three-dimensional visualization, respectively, for radial pattern one. Here a central island of relatively sensitive retinal function is surrounded by paracentral relative scotoma. (**C**, **D**) The point map and three-dimensional visualization, respectively, for a second custom simulated threshold pattern with an altered distribution of point sensitivities. Here the paracentral regions are relatively preserved and a central scotoma present. Both examples have been designed with an equal mean sensitivity of 17 dB to illustrate a significant underestimate of retinal sensitivity in the second radial pattern when using mean sensitivity alone to interpret the plots.

sensitivity, however, begins to break down and suffer from an induced averaging method floor effect when only a few retinal loci are sensitive across the testing grid (Fig. 5A, week 5). Figure 5C demonstrates this effect where mean sensitivity reaches zero decibels with volume retaining a nonzero value. The nonzero volume corresponds to contributions by the few remaining points of retinal sensitivity that the averaging in a mean sensitivity index did not detect (as also seen in Fig. 4C).

Radial or Nonuniform Grid Patterns—Simulated Examples

To investigate nonuniform grid patterns, two distinctly different simulated test cases were designed with identical mean sensitivity values. Radial pattern one (Fig. 6A) represents a relatively preserved central island surrounded by relative scotoma in the paracentral regions. This is analogous to retinal sensitivities seen in choroideremia or *RPGR*-related retinitis pigmentosa. Radial pattern two (Fig. 6C) represents relative central scotoma with preserved paracentral regions, similar to that seen in geographic atrophy or macular dystrophies. Plotting the three-dimensional hill of vision for both cases (Figs. 6B, 6D) highlights that despite having identical mean sensitivity values, significant differences in sensitivity volumes are obtained (9683 dB-degrees^2 and 13,571 dB-degrees^2 in radial tests one and two, respectively). This equates to a 29% difference in volume between the two examples. Converting this percentage change back to a decibel scale implies that a more accurate measure of the mean sensitivity in radial test 2 would be approximately 22dB, rather than the 17dB given by a simple averaging method. This discrepancy is due the lower sampling density of points in the paracentral regions. A single high value point sensitivity here has far less impact on an overall mean than several high-value sensitivity points covering a theoretically similar area in the more densely sampled central region.

Discussion

In this study we introduce a method for the production of microperimetry three-dimensional hill of vision plots. To our knowledge, this study represents the first application of the generalized microperimetry hill of vision method to a cross-section of ocular pathologies using a web application or freely available, open-source software. It also explicitly investigates the impact in nonuniform grid patterns within microperimetry. Furthermore, we demonstrate the increased accuracy of this three-dimensional hill of vision method in detecting retinal sensitivity changes in patients who have advanced vision loss compared with the common standard mean decibel value using a patient case study.

The VFMA method has demonstrated success in both observational studies and clinical trials. We have verified our method against the VFMA method implemented by Weleber. Both techniques show similar outcomes and patterns. The small difference in the numerical values may be as a result of algorithmic differences, however, the direction and pattern of loss is qualitatively equivalent with excellent quantitative agreement using ICC analysis. R programming language is a freely available tool used by data scientists and researchers. The inclusion of several R-packages allows for a relatively simple routine to be adopted to convert raw data files from the MAIA microperimeter into three-dimensional hill of vision plots with an associated volume measure. The development of an R-package, webapp and open-source code promotes open science enabling independent validation, increase research repeatability and allows for user modifications and further development tailored to specific analysis requirements. Our use of decibels degrees squared also provides clinicians with a more intuitive and familiar unit scale. The three-dimensional output provides a detailed visualization of retinal sensitivity with subtle topographical changes more easily detected than the current two-dimensional MAIA output, particularly when used interactively. A volume measure also provides a wider range metric for retinal sensitivity than mean sensitivity and does not suffer from an induced averaging floor effect as such hill of vision and volumetric approaches in microperimetry have been used to good effect in previous clinical trials.[9,10] A potentially useful additional aspect of three-dimensional hill of vision representation in microperimetry may be the study of gradients across scotoma borders in ocular pathologies. Strong structure-function correlations have been found using static-perimetry hill of vision gradient measures in autosomal dominant retinitis pigmentosa.[8] A detailed assessment of gradients across borders may be a promising tool for sensitive measures of disease progression or an early marker for novel treatment efficacy. For example, it is known that in *RPGR*-related retinitis pigmentosa, functional field loss progresses in a radial fashion from mid-peripheral locations resulting in a gradual decline in retinal sensitivity. There is a relatively shallow gradient from central healthy locations to more affected paracentral regions. In contrast, in choroideremia patients, the gradient from healthy central regions to more affected paracentral areas is often far steeper.

Three dimensional representations help to visualize these pathology specific characteristics and gradient measures may allow for more sensitive measures of functional retinal changes. We anticipate that potential future adoption of adaptive optics microperimetry will greatly enhance our understanding of retinal function at scotoma borders in ocular pathology and three-dimensional visualization will be an invaluable tool to conceptualize gradient properties at these borders.

We propose that the production of a three-dimensional hill of vision representation of MAIA results is now achievable to a wider range of clinical researchers. A volume measure of the hill of vision combines the extent and degree of retinal sensitivity and allows for a simpler visualization of subtle changes in retinal sensitivity function. In addition, the resulting volume of the hill of vision allows for the utilization of the full dynamic range of the microperimeter whilst retaining the attributes of a single value index. This is valuable in patients close to end stage disease where the mean sensitivities may approach the floor of the machines' capability. In particular, for radially or irregularly spaced grid testing patterns, mean sensitivity is problematic. We emphasize that the use of mean sensitivity in these instances poses a significant potential for error in assessing retinal sensitivity function and that mean values can only be representative of function in evenly spaced grid patterns. For radial or unequally spaced patterns, mean values are weighted towards those points located in more densely spaced regions. Consequently, uniform testing grids such as the 10-2 grid, are typically used in clinical trials. A global volumetric measure can be used without similar issues. Volumetric data are able to model sensitivity information in sparse regions by interpolating values between tested points and use these data to inform an overall sensitivity measure. This benefit may subsequently permit the use of nonuniform testing grids with higher sampling density in regions of particular clinical interest, for example, at the border of a scotoma. Theoretically, nonuniform grids may also be uniquely tailored to the pathology of each patient, for example, in the unique scalloped islands of choroideremia patients, with a volumetric measure still being comparable between subjects where mean sensitivity would not be. In the context of novel treatments, the three-dimensional hill of vision and wide volume range allows for simpler detection of localized changes in retinal sensitivity, where the mean sensitivity may be relatively unchanged. This may be of use in detection of progression during the natural history of the disease or in response to novel therapies where a pointwise analysis may otherwise be employed. Further work in providing an age-matched normative database may further expand the clinical application of fundus tracked perimetry devices. Importantly, we demonstrated in this study the value of volumetric measures as a safety signal in inflammation after novel treatments.

In conclusion, volumetric measures of retinal sensitivity confer several advantages over the standard output of mean sensitivity in microperimetry, most significantly in avoidance of the averaging floor effects. These are especially relevant in diseases affecting the central retina, both inherited and acquired, which produce a central scotoma and in whom with disease progression the mean sensitivity will tend towards zero decibels. Further avenues of investigation include characterizing the natural history of volumetric sensitivity in specific retinal diseases; performing direct comparisons between uniform and nonuniform testing grids and the resultant volume measures; as well defining disease specific test-retest variability and analyses of gradients across scotoma borders. Here, we present methodology and novel open-source software to allow user-generated detailed interactive three-dimensional microperimetry hill of vision plots with volumetric sensitivities and suggest that they may form an appropriate clinical trial outcome measure.

Acknowledgments

The authors thank the kind donation made by Jean Williams (known as the Winstanley donation) to the University of Oxford for research into inherited macular diseases.

Supported by the NIHR Oxford Biomedical Research Centre. Jasleen K Jolly is funded by the National Institute for Health Research (NIHR) [Clinical Doctoral Research Fellowship CA-CDRF-2016-02-002], and the Winstanley Fund. Jasmina Kapetanovic is funded by the National Institute for Health Research (NIHR) and Global Ophthalmology Awards Fellowship, Bayer.

Disclosure: **A.S. Josan,** None; **T.M.W. Buckley,** None; **L.J. Wood,** None; **J.K. Jolly,** None; **J. Cehajic-Kapetanovic,** None; **R.E. MacLaren,** None

References

1. Muthusamy V, Turpin A, Walland MJ, Nguyen BN, McKendrick AM. Increasing the spatial resolution of visual field tests without increasing test

duration: An evaluation of ARREST. *Transl Vis Sci Technol*. 2020;9(13):24.
2. Traquair HM. *An introduction to clinical perimetry*. St. Louis: The C V Mosby Company; 1949.
3. Weleber RG, Smith TB, Peters D, Chegarnov EN, Gillespie SP, Francis PJ, et al. VFMA: Topographic analysis of sensitivity data from full-field static perimetry. *Transl Vis Sci Technol*. 2015;4(2):14.
4. Weleber RG, Tobler WR. Computerized quantitative analysis of kinetic visual fields. *Am J Ophthalmol*. 1986;101:461–468.
5. Weleber RG, Pennesi ME, Wilson DJ, et al. Results at 2 years after gene therapy for RPE65-deficient leber congenital amaurosis and severe early-childhood-onset retinal dystrophy. *Ophthalmology*. 2016;123:1606–1620.
6. Birch DG, Bernstein PS, Iannacone A, et al. Effect of oral valproic acid vs placebo for vision loss in patients with autosomal dominant retinitis pigmentosa: A randomized phase 2 multicenter placebo-controlled clinical trial. *JAMA Ophthalmol*. 2018;136:849–856.
7. Wagner SK, Jolly JK, Pefkianaki M, et al. Transcorneal electrical stimulation for the treatment of retinitis pigmentosa: results from the TESOLAUK trial. *BMJ Open Ophthalmol*. 2017;2(1):e000096.
8. Smith TB, Parker M, Steinkamp PN, Weleber RG, Smith N, Wilson DJ. Structure-function modeling of optical coherence tomography and standard automated perimetry in the retina of patients with autosomal dominant retinitis pigmentosa. *PLoS One*. 2016;11(2):e0148022.
9. Tanna P, Georgiou M, Aboshiha J, et al. Cross-sectional and longitudinal assessment of retinal sensitivity in patients with childhood-onset Stargardt disease. *Transl Vis Sci Technol*. 2018;7(6):10.
10. Mehat MS, Sundaram V, Ripamonti C, et al. Transplantation of human embryonic stem cell-derived retinal pigment epithelial cells in macular degeneration. *Ophthalmology*. 2018;125:1765–1775.
11. Dimopoulos IS, Tseng C, MacDonald IM. Microperimetry as an outcome measure in choroideremia trials: Reproducibility and beyond. *Invest Ophthalmol Vis Sci*. 2016;57:4151–4161.
12. Charng J, Sanfilippo PG, Attia MS, et al. Interpreting MAIA microperimetry using age- and retinal loci-specific reference thresholds. *Transl Vis Sci Technol*. 2020;9:19.
13. Denniss J, Astle AT. Spatial interpolation enables normative data comparison in gaze-contingent microperimetry. *Invest Ophthalmol Vis Sci*. 2016;57:5449–5456.
14. Team RC. *R: A language and environment for statistical computing*. Vienna, Austria: R Foundation for Statistical Computing; 2020.
15. Cehajic-Kapetanovic J, Xue K, Martinez-Fernandez de la Camara C, et al. Initial results from a first-in-human gene therapy trial on X-linked retinitis pigmentosa caused by mutations in RPGR. *Nat Med*. 2020;26:354–359.
16. Weijland A, Haag-Streit AG. *Automated perimetry: visual field digest*. Köniz/Bern: Haag-Streit AG; 2004.
17. Smith TB, Smith N, Weleber RG. Comparison of nonparametric methods for static visual field interpolation. *Med Biol Eng Comput*. 2017;55:117–126.
18. Duchon J. Interpolation des fonctions de deux variables suivant le principe de la flexion des plaques minces. *ESAIM: Mathematical Modelling and Numerical Analysis. Modélisation Mathématique et Analyse Numérique*. 1976;10:5–12.
19. Nychka D, Furrer R, Paige J, Sain S. Fields: Tools for spatial data. 2017, R package version 11.6, https://github.com/NCAR/Fields.
20. Wickham H. *ggplot2: Elegant Graphics for Data Analysis*. New York: Springer-Verlag; 2016.
21. Adler D, Murdoch D. Package "rgl." 2017. Available at http://mirror.nju.edu.cn/pub/CRAN/web/packages/rgl/rgl.pdf.
22. Christoforidis JB. Volume of visual field assessed with kinetic perimetry and its application to static perimetry. *Clin Ophthalmol*. 2011;5:535–541.
23. Heijl A, Krakau CE. An automatic perimeter for glaucoma visual field screening and control. Construction and clinical cases. *Albrecht Von Graefes Arch Klin Exp Ophthalmol.* 1975;197(1):13–23.